A SYNERGY CODE IN CO-PYROLYSIS

ILLE JOHANNES[*], VILJA PALU

Tallinn University of Technology
Department of Polymeric Materials
Laboratory of Oil Shale and Renewables Research
Ehitajate tee 5, 19086 Tallinn, Estonia

Abstract. *For the first time, a mathematical model has been proposed to describe the influence of blending ratio on the synergy in co-pyrolysis. The model is based on the stability of a new cross-compound A_nB formed between the pyrolysis products of the blend components. A new characteristic, named synergy factor (δ), has been introduced to express the synergy formula. The value of δ and synergy in oil yield are positive when A_nB is volatile or soluble in the solvents applied for oil separation. As an example, the model deduced was proved in the mathematical processing of earlier published experimental results on the co-pyrolysis of oil shale and pine wood in supercritical water at 380 °C during 4 hours. The values of δ were estimated for the subsequent distribution of the pyrolysate into water extract (including ether soluble and insoluble extracts), water insoluble oil (including benzene and acetone extracts), solid residue, and gas and pyrogenetic water.*

Keywords: *co-pyrolysis, mathematical modeling, synergy, synergy factor, oil shale, pine wood, autoclave.*

1. Introduction

Much attention has been paid to the co-pyrolysis of fossil fuels with biomass (BM) [1–15] and plastic wastes (PL) [15–26] with the aim to expand the crude resources and flexibility, to improve the composition of liquid products, and to advance environmental sustainability.

It is understandable that the co-pyrolysis of fossil fuels with PL consisting mainly of hydrocarbons and having a higher individual decomposition degree should upgrade the oil composition and increase the oil and/or gas yield. At that, the hydrogen transformation between the components would give an additional increase in the yield of volatiles. In contrast, the heteroatoms (O, N and S) typical of BM can deteriorate the composition and heating value of the products, whereas the mineral part of fossil fuels can

---

[*] Corresponding author: e-mail *ille.johannes@ttu.ee*

decrease the emission of toxic NO_x, SO_x, and organic volatiles as a sorbent, or act as a cracking catalyst. Besides, BM being CO_2-neutral has an added attractiveness in the context of increasingly stringent CO_2 emission laws.

Several researchers have published experimental results concerning interactions between the blend components in co-pyrolysis. The data revealing higher or lower yields of decomposition products than expected from the additive proportional contributions (the so-called positive or negative synergy) are conflicting because the effect depends on the type and contact of components, pyrolysis duration, temperature and heating rate, removal of or equilibrium between the volatiles formed, presence of solvents, catalysts and H-donors.

1.1. Co-pyrolysis of fossil fuels with BM

Most co-pyrolysis studies have been devoted to coal/BM blends. The results have been mainly obtained in thermogravimetric analysis (TGA) where less than some tens of grams of samples are used.

It is known that the temperature of BM thermal decomposition is about a hundred degrees centigrade lower than that of coal. There are plenty of papers reporting that the position of peaks and the shape of TGA curves of the two components remain unaltered in blends. So, no interactions have been found in TGA during the co-pyrolysis of coal in blends with agricultural BM or wood waste [1−5], and Thai lignite with corncob [6]. The lack of the synergetic effect in the blends of coal with switchgrass was also proved in a drop reactor at 900 °C [7]. Similarly, no obvious synergy was observed by Jones et al. [8] in pyrolysis-GC-MS of coal/pine blends, and of model hydrocarbon/coal and BM/coal blends.

Inversely, it was reported in [9] that the TGA method from ambient to 900 °C for 10% of hazelnuts in the blend with different rank coals revealed considerable deviations from the theoretical char yields in the case of peat and lignites. At that, the presence of hazelnuts increased the char yield with peat and decreased considerably that with lignites. Also, it was revealed that the char yield decreased and the liquid yield increased compared with the calculated values in the fast co-pyrolysis of legume straw with Dayan lignite [10]. The experiments were performed in a free fall reactor (i.d. 20 mm, length 1800 mm) heated in the range of 500 to 700 °C. In the free fall reactor, both the higher blending ratio (around 70 wt% of BM) and the relatively lower temperature (around 600 °C) were more in favour of obvious synergies during the co-pyrolysis of BM/coal blends.

As a rule, non-additive compositions and yields of pyrolysis products were observed under low heating rates characteristic of large-scale batch pyrolysis tests. For example, in the co-pyrolysis of 100 grams of bituminous coal/pine wood blends at 520 °C [8] the oil contained less aliphatic and aromatic hydrocarbons and more phenols than would be expected from additive behavior. The co-pyrolysis of coal and BM in briquettes at 600 °C had a synergetic effect on the desulphurization of coal [11]. Park et al. [12]

showed in a fixed bed reactor the maximum synergy to produce 6% more gas and 3% less char at a wood/coal blending ratio of 2/3. Sonobe et al. [6] reported that in the fixed bed pyrolysis the char yield from the 1/1 blend of lignite/corncob was also 9% lower than the calculated value. The enhanced devolatization of pyrolysis products from the blend was explained by the transfer of hydrogen from corncob to lignite, as well as the promotion of the low-temperature thermal decomposition of lignite by exothermic heat release from corncob pyrolysis.

According to [13] a significant synergy could be obtained during a rapid co-pyrolysis of the BM/coal blend in a high-frequency furnace where both the high heating rate and the satisfying contact between fuel particles were ensured. However, increasing the share of BM, whose packing density and thermal conductivity were lower than those of coal, decreased the heating rate of blends and weakened the synergies. Noteworthy is that contrary to the fall reactor [10], a low BM/coal mass ratio resulted in significant synergies during the rapid co-pyrolysis, leading to an increase in volatiles.

It was found in [14] that the co-pyrolysis of woody BM and waste tires with catalysts in a fixed-bed reactor revealed an essential synergetic effect. The yields of carbon and hydrogen from the initial blend, and also the H/C atomic ratio in the oil were higher than calculated. It was concluded that in co-pyrolysis the hydrogen transfer inhibited the formation of polycyclic aromatic hydrocarbons from tires whereas the catalysts applied had an insignificant effect on the synergy. A positive synergy in the oil yield was also proved in the co-pyrolysis of scrap tires and Turkish Mustafa Kemal Pasa lignite [15].

1.2. Co-pyrolysis of fossil fuels with PL

Sharypov et al. [16] co-processed Russian Kansk-Achinsk brown coal with PL, using TGA and autoclavic pyrolysis. In this work, TGA under argon atmosphere established clearly non-additive mass loss for the blends. The highest increase in transformation degree (10–13% of calculated) was observed when the coal share was below 30%. In autoclaves, a non-additive increase in the conversion degree of coal/PL blends was observed in the whole range of the feedstock composition, and a maximum of synergy (10–15%) was observed for the 1/1 blend. The increase was attributed to the improvement in coal conversion as the conversion of PL alone under the conditions tested was close to 100%, already.

Independent thermal behavior with no synergy at all ratios was revealed in the TGA investigations of woody BM (beech, pine, cellulose, hydrolytic lignin) with PL (polyethylene, polypropylene) [17, 18]. Pyrolysing the same blends in autoclaves at 400 °C the yields of products were additive in the range of 50 to 100% BM. When the BM content was lower than 50%, non-additive phenomena occurred, leading to higher yields of light fractions. At that, the origin of BM, as well as the type of polymers played an important role in the final distribution of products. The non-additive increase in the

conversion degree and yields of distillable fractions was also proved in the co-hydropyrolysis (H_2 3 MPa, 400 °C) of pine wood with PE or PP in auto-claves [19].

Results of TGA on the thermal decomposition of blends from Chinese Shenfu (SF) and Huayingshan (HYS) coals with PL showed a negative synergy in case of oxygen rich SF (O^{daf} = 12%) with both LDPE and HDPE, and a positive synergy in case of the blends of HYS (O^{daf} = 2%) only with HDPE [20].

Suelves et al. [21] co-pyrolyzed 2–5 mg of 70/30, 50/50 and 40/60 blends (%) of Samca coal and aliphatic C_{50} (pentacontane) at 900 °C in a pyroprobe 1000 CDS. A positive synergy was reported in the yields of CO, C_2H_6, C_2H_4, C_4H_6 for all the blends, and a negative one in those of C_3H_8, C_4H_8 and C_6-compounds for the 40/60% blends. Synergetic effects of aromatics (benzene, toluene xylene and alkylbenzene) were negative for the 50/50 blend, but positive for the 70/30.

1.3. Co-pyrolysis of oil shales with PL and BM

There have been only a few works concerning co-pyrolysis of oil shale with BM or PL, despite that oil shales can be a valuable potential source of liquid hydrocarbons in several countries.

In the works of Tiikma et al. [22, 23] the effect of co-pyrolysis of LDPE with Estonian Kukersite oil shale, its semicoke and Dictyonema argillite on the yield and composition of the pyrolysis oil was investigated. The yields of pyrolysis products (gas, oil, solid residue) of Kukersite/PL blends practically coincided with those calculated from the partial contribution of the blend components. Dictyonema argillite acted as a catalyst increasing the yields of gas and light oil fractions, and decreased that of heavier oil fractions.

On the contrary, according to Aboulkas et al. [24, 25], the co-pyrolysis of HDPE, LDPE and PP with Moroccan oil shale from the Tarfaya deposit (1/1) had a significant synergy leading to an increase in thermal stability in TGA whereas in an autoclave, the positive synergy in the conversion degree of the blends varied between 2.4 and 6.0%, without noteworthy rules. In the 1/1 blends the maximum values of synergy in oil yields reached 4.0% for HDPE, 4.7% for LDPE and 5.2% for PP at 500–525 °C.

Veski et al. [26] have investigated the co-pyrolysis of Estonian oil shale Kukersite and pine wood (0, 25, 54, 75 and 100% of BM in the blend on OM basis) in supercritical water (380 °C, 4 h). It was found that the yields of different extraction fractions of oil were 1.5–1.9 times higher, and the yields of gas, water and solid residue 0.5–0.8 times lower than the corresponding additive values. It was revealed that the rise in the oil yield resulted from addition of polar compounds only and depended on the ratio of the blend components.

The bio-oils formed represent a highly oxygenated complex mixture of large size polymolecules of esters, ethers, aldehydes, ketones, phenols, carboxylic acids and alcohols [27].

The above-described interactions affording non-additive yields, and characteristics of co-pyrolysis products have not been mathematically modeled before.

The aim of this work was to create a common mathematical approach for calculation, prediction and comparison of synergies in co-processing products at any ratio of the blend components.

The mathematical approach proposed is explained and proved based on the experimental data published earlier by Veski, Palu and Kruusement [26].

2. Mathematical modeling of synergy in co-pyrolysis

A common formula for synergy (Δ) is expressed as follows:

$$\Delta = y_{\exp} - y_{ad}, \tag{1}$$

where $y_{\exp}$ is the experimental value of any characteristic output of co-pyrolysis products (yield of gas, extracts, solid residue, viscosity, density, boiling point, etc.), and y_{ad} is the value of any characteristic output of the products calculated by addition of the proportional contributions of individual components.

In this work, a hypothesis is developed that the synergy in co-pyrolysis is caused by formation of a new cross-compound A_nB between the solid and liquid pyrolysis products of individual blend components A and B according to the following equilibrium reaction:

$$nA + B \leftrightarrow A_nB \tag{2}$$

A positive synergy in the oil and gas yields can arise when one of the reactants, A or B, comes from the solid residue, and A_nB is volatile in open retorts and extractable in closed devices. A negative synergy in the oil yield and a positive one in the yield of solid residue appear when A_nB is non-volatile or insoluble in the solvents applied for oil extraction. The value of n indicates the apparent number of A moles required for the reaction with one mole of B.

The stability constant (K) for a complex formation according to the reaction equation (2) is described by the activities (a_i) of components as follows:

$$K = a_{AB} / (a_A{}^n a_B) \tag{3}$$

The activities can be approximately expressed through activity constants (γ_i), yields of the pyrolysis products from individual components (Δ, y_{A1}, $y_{B1,SR}$), the mole masses of the products (M_i), and share masses (g_i) of OM of the components in the blend called blending ratios ($x_A = g_A/(g_A + g_B)$ and $x_B = g_B/(g_A + g_B)$) as follows:

$$a_{AB} = \gamma_{AB} \Delta / M_{AB} \tag{4}$$

$$a_A = \gamma_A \, y_{A1} \, x_A / M_A \tag{5}$$

$$a_B = \gamma_{B,SR} \, (y_{B1,SR}) \, x_B / M_{B1,SR} \tag{6}$$

The index B1,SR in Equation (6) indicates that the characteristics belong to the solid residue in the pyrolysis of the individual component B. Here and below, the analogous characteristics of the component A and the synergy product A_nB may belong to a variety of pyrolysis products (gas, various extracts), and a particular product is described in the text.

The yield of the new complex leading to synergy is described, congregating the invariables according to their type as follows:

$$\Delta = \{K(\gamma_A \gamma_{B,SR}/\gamma_{AB}) \, [M_{AB}/(M_A{}^n M_B)][\, y_{A1}{}^n (y_{B1,SR})]\}(x_A)^n x_B \tag{7}$$

Supposing that the values of activity constants, mole masses, and yields estimated for the individual components ($x_i = 1$), and the unknown values of M_i are constant at any blend composition under the same operation conditions, Equation (3) can be expressed as a simple proportionality between synergy and product of the shares of components:

$$\Delta = \delta_{n,1} \, (x_A)^n x_B \tag{8}$$

Noteworthy is that here we have introduced a new constant named "synergy factor" and marked as $\delta_{n,1}$. The index of the factor shows the exponents of the shares x_A and x_B and n is the number of moles of the first component in the reaction with one mole of the second component. The synergy factor consists of several constant values as follows:

$$\delta_{n,1} = K(\gamma_A \gamma_{B,SR}/\gamma_{AB}) \, [M_{AB}/(M_A{}^n M_B)][\, y_{A1}{}^n (y_{B1,SR})] \tag{9}$$

The synergy factor enables quantitative description and comparison of the impact on the synergy of different components of the blend, their ratios and pyrolysis conditions. Equation (9) indicates that δ is valid only under definite pyrolysis conditions because y_i depends on temperature and duration, and K on temperature. There is no synergy when $\delta = 0$. When an equimolar reaction takes place, $n = 1$, and the maximum synergy is 0.25δ as far as $x_A = x_B = 0.5$. Any shift of the maximum from the blend ratio 0.5 demonstrates that the reaction is not equimolar.

When $n = 1$, Equation (8) represents a simple proportionality:

$$Y = bX, \tag{10}$$

where $Y = \Delta$, $X = x_A x_B$ and $b = \delta_{1,1}$.

So, an equimolar synergy reaction is proved when a straight line crossing zero is obtained when the experimental results are depicted according to Equation (10). In this case, it is easy to find the synergy factor $\delta_{1,1}$ from the plot of Δ versus $x_A x_B$.

When a polymolar synergy reaction takes place, the values of $\delta_{n,1}$ and n can be found from the reciprocal and slope of the linear relationship obtained logarithming Equation (8):

$$Y = b_0 + b_1 X, \tag{11}$$

where $Y = \ln(\Delta / x_B)$, $X = \ln(x_A)$, $b_0 = \ln \delta_{n,1}$, and $b_1 = n$. So, $\delta_{n,1} = \exp(b_0)$.

The synergy characteristics estimated under different pyrolysis conditions would help to understand, describe and compare the effects of various factors as temperature, heating regime, solvents, catalysts and reactor type on synergistic effects.

3. Experimental

In this work, the mathematical model proposed above was elaborated and proved taking experimental data from [26] where the results concerning co-pyrolysis of oil shale (50.5% OM^d, 12.8% $CO_2{}^d{}_{min}$, 37.2% A^d, and 0.6% hygroscopic water) and pine wood (99.6% OM^d, 0.4% A^d and 9.1% hygroscopic water) were published for the first time. The liquefaction was carried out under conditions of supercritical water, heating up during 110 min to 380 °C, and duration at the nominal temperature of 4 hours. A series of experiments were conducted using 60 grams of each blend (0, 25, 54, 75 and 100% of wood OM in the blend OM) and 180 grams of water in a 500 cm^3 autoclave. The pyrolysate was subsequently separated into the water extract (including ether soluble (E) and insoluble extracts (W)), water insoluble oil (including benzene (B) and acetone (A) extracts), solid residue (SR), and gas and pyrogenetic water (G + w) found from difference. The yields of the products are presented in Table 1. The group composition of the benzene extract was estimated by thin-layer chromatography. The results are given in Table 2.

A more detailed characterization of samples, procedures and products is given in [26].

Table 1. Experimental yields of products, % of **OM [26]**

Product	Symbol	Wood OM in blend OM, %				
		0	25	54	75	100
Water soluble oil, incl.	W+E	7.7	7.6	8.9	11.8	5.6
soluble in ether	E	3.0	3.3	5.2	7.0	4.6
insoluble in ether	W	4.7	4.3	3.7	4.8	1.0
Water insoluble oil, incl.	B+A	55.7	67.0	48.6	38.3	10.3
soluble in benzene	B	53.2	63.7	39.8	33.5	6.0
soluble in acetone	A	2.5	3.3	8.8	4.8	4.3
Solid residue	SR	6.5	7.1	12.6	16.1	32.2
Gas and pyrogenetic water	G+w	30.1	18.3	29.9	33.8	51.9

Table 2. Group composition of benzene extract, % [26]

Group of compounds		Wood OM in blend OM, %				
		0	25	54	75	100
1	High polar heterocompounds	52.9	66.6	70.6	71.9	63.9
2	Neutral heterocompounds	20.4	18.9	14.0	16.6	17.1
3	Polyaromatic hydrocarbons	19.4	8.6	10.0	7.9	8.4
4	Monoaromatic hydrocarbons	1.2	1.3	2.2	1.2	2.7
5	Nonaromatic hydrocarbons	6.1	4.6	4.3	2.4	8.0

4. Data processing and discussion

4. 1. Estimation of synergy factors using the second-order polynomial trendlines

Below, for a better understanding of the new approach the data processing will be described in detail.

With the aim to eliminate experimental errors in calculations of the synergies representing small differences between comparatively high values, the experimental yields given in Table 1 were smoothed using the stochastic second-order polynomial trendlines:

$$Y_{exp} = b_2 x_B{}^2 + b_1 x_B + b_0 \qquad (12)$$

Analogous polynomials were applied for approximation of the yields of products soluble in different organic solvents, and of the group composition of benzene soluble compounds in [26]. The plots of experimental yields of co-pyrolysis products and their trendlines versus blend composition are presented in Figure 1.

The regression coefficients of the adjunct trendlines in Figure 1 for inter-polation of the experimental yields according to Equation (12) were obtained using Excel Data Processing. The data are given in Table 3.

Table 3. Regression coefficients of the second-order polynomial trendlines in Fig. 1

Product [1]	b_2	b_1	b_0
G+w	62.07	−38.2	28.4
W+E	−12.19	12.13	6.83
B+A	−85.41	37.33	57.76
B	−71.8	21.53	55.82
E	−6.07	8.81	2.47
SR	35.53	−11.28	7.01

[1] Symbols see in Table 1.
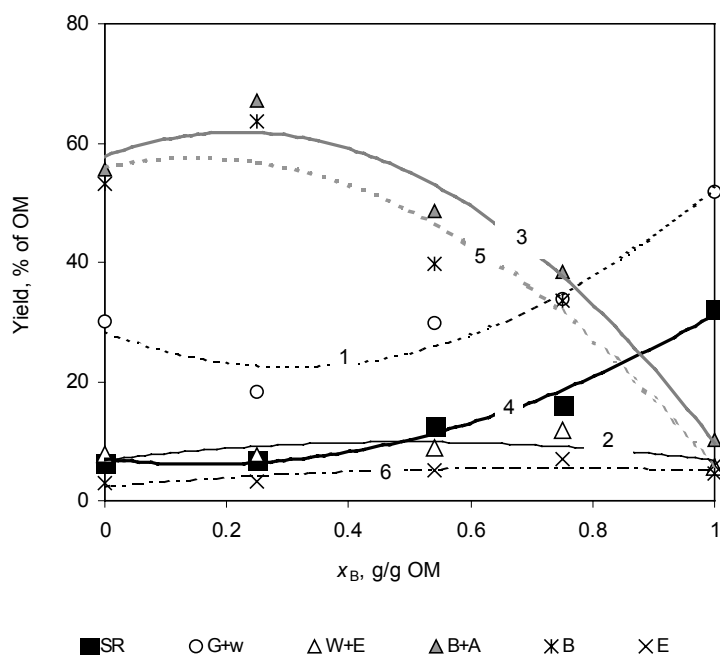
Fig. 1. Effect of blend composition on the yield of co-pyrolysis products: 1 – (G + w), 2 – (W + E), 3 – (B + A), 4 – SR, 5 – B, 6 – E. Points illustrate experimental yields, curves depict the yields predicted by the second-order polynomial trendlines.

The coefficients in Table 3 were applied for interpolating the experimental yields of products with a step 0.1 g/g of wood in the blend. The respective additive yields were calculated as follows:

$$y_{ad} = x_A y_{A1} + x_B y_{B1} \tag{13}$$

The values of interpolated experimental and additive yields and their differences are presented in Table 4.

The plots of synergies from Table 4 versus the products $x_A x_B$ depicting Equation (8) for $n = 1$ are shown in Figure 2. It can be concluded from the satisfactory agreement between the experimental points and the linear trendlines that equimolar reactions take place in the synergies revealed.

The equimolar synergy factors for the co-pyrolysis of oil shale and pine wood in supercritical water and their standard errors estimated as slopes of trendlines in Figure 2 are given in Table 5.

Table 4. Effect of blend composition (g/g) on the yield and synergy of pyrolysis products, % of OM

Blend composition											
x_B	0.0	0.1	0.2	0.3	0.4	0.5	0.6	0.7	0.8	0.9	1.0
Experimental interpolated yields											
G+w	30.10	25.20	23.24	22.53	23.05	24.82	27.83	32.07	37.56	44.30	51.90
W+E	7.70	7.92	8.77	9.37	9.73	9.85	9.72	9.35	8.73	7.87	5.60
B+A	55.70	60.64	61.81	61.27	59.03	55.07	49.41	42.04	32.96	22.17	10.30
SR	6.50	6.24	6.18	6.82	8.18	10.25	13.03	16.52	20.73	25.64	32.20
B	53.2	57.26	57.25	55.82	52.94	48.64	42.89	35.71	27.09	17.04	6.0
E	3.0	3.29	3.99	4.57	5.02	5.36	5.57	5.66	5.63	5.48	4.6
Yields calculated by additive contributions											
G+w	30.10	32.28	34.46	36.64	38.82	41.00	43.18	45.36	47.54	49.72	51.90
W+E	7.70	7.49	7.28	7.07	6.86	6.65	6.44	6.23	6.02	5.81	5.60
B+A	55.70	51.16	46.62	42.08	37.54	33.00	28.46	23.92	19.38	14.84	10.30
SR	6.50	9.07	11.64	14.21	16.78	19.35	21.92	24.49	27.06	29.63	32.20
B	53.2	48.48	43.76	39.04	34.32	29.60	24.88	20.16	15.44	10.72	6.0
E	3.0	3.16	3.32	3.48	3.64	3.80	3.96	4.12	4.28	4.44	4.6
Synergies											
G+w	0.00	−7.08	−11.22	−14.11	−15.77	−16.18	−15.35	−13.29	−9.98	−5.42	0.00
W+E	0.00	0.43	1.49	2.30	2.87	3.20	3.28	3.12	2.71	2.06	0.00
B+A	0.00	9.48	15.19	19.19	21.49	22.07	20.95	18.12	13.58	7.33	0.00
SR	0.00	−2.83	−5.46	−7.39	−8.60	−9.10	−8.89	−7.97	−6.33	−3.99	0.00
B	0.00	8.78	13.49	16.78	18.62	19.04	18.01	15.55	11.65	6.32	0.00
E	0.00	0.13	0.67	1.09	1.38	1.56	1.61	1.54	1.35	1.04	0.00
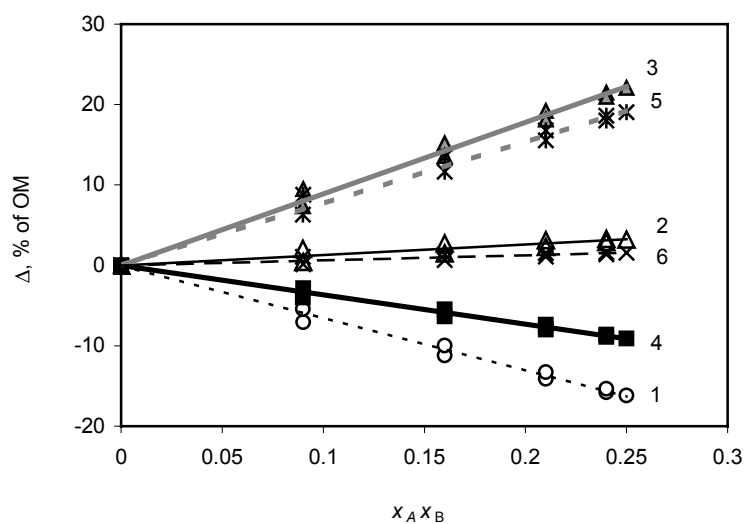
Fig. 2. Trendlines to estimate equimolar synergy factors for the co-pyrolysis products (symbols see in Fig. 1).

Table 5. Equimolar synergy factors for the yields of co-pyrolysis products

Product	G + w	W + E	B + A	SR	B	E
$\delta_{1,1}$, %(g/g)$^{-2}$	−65.4	12.9	89.0	−36.6	77.2	6.3
Standard error, ±%	0.9	0.9	1.2	0.6	1.4	0.5

The data in Table 5 show a vital positive synergy (maximum 22% (calculated as $0.25\delta_{1,1}$) in the 1/1 blend) for the summary yield of oil (benzene and acetone extracts) caused mainly (19%) by the synergy in the benzene extract. The favourable increase of oil yield is balanced by negative synergies, −16% and −9%, in the yields of gas and pyrolytic water, and solid residue.

4.2. Prediction of the yields of co-pyrolysis products using an equimolar synergy model

The actual yields of products were predicted as follows:

$$y_{exp} = \delta_{1,1}x_A x_B + x_A y_{A1} + x_B y_{B1} \tag{14}$$

Figure 3 depicts the experimental results from Table 1 and the curves predicted using Equation (14).

Noteworthy is that the curves in Figure 3 predicted using Equation (14) actually coincide with the polynomial trendlines in Figure 1. The advantage of the model applied in Figure 3 is manifested by its physico-chemical meaning and the requirement for only one coefficient, $\delta_{1,1}$, enabling a simple comparison of synergies in various characteristics and in prediction of the effects of blending ratios. Nevertheless, the stochastic polynomials were useful in the stage of research work, just for elimination of experimental errors in estimation of δ. So, it is important to find a suitable adjunct trendline for interpolation of experimental data.

Any deviation of experimental yields from the second-order trendlines may result from either experimental errors or the complicated nature of the process. In the latter case a higher-order polynomial trendline should be applied instead of Equation (11). As seen in Figure 3, dispersions are the most troubling for the products B + A (curve 3), B (curve 5) and G + w (curve 1).

4.3. Estimation of synergy factors using the fourth-order polynomial trendlines

As an example, the fourth-order polynomial was applied to interpolation of the experimental yields of fractions Gas + w, B + A and B having considerable deviations from the second-order trendlines. The regression coefficients found by means of the respective Excel trendlines for the data in Table 1 are given in Table 6.
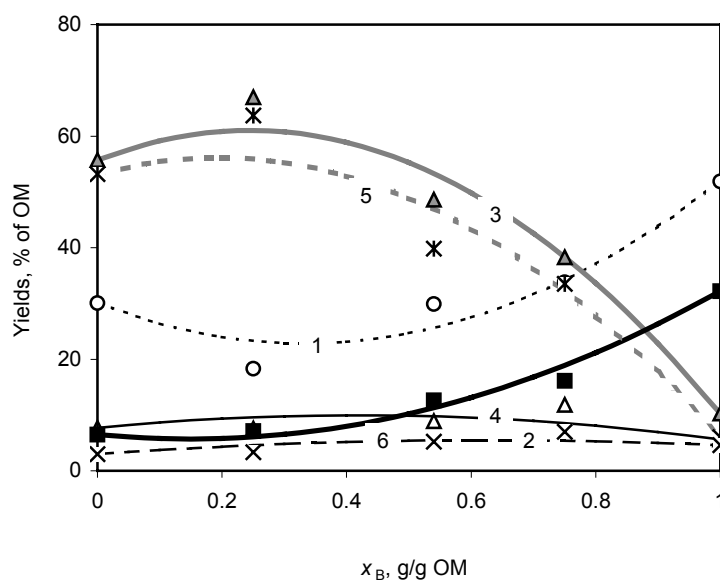
Fig. 3. Effect of blend composition on the yield of co-pyrolysis products assuming equimolar synergy reactions. Points illustrate experimental yields, curves depict the yields predicted according to Equation (14) (symbols see in Fig. 1).

Table 6. Regression coefficients of the fourth-order polynomial trendlines for the yields of products in Table 1

Product	b_4	b_3	b_2	b_1	b_0
G + w	486	−1020	730	−174	30.1
B + A	−527	1119	−827	190	55.7
B	−818	1708	−1179	243	53.2

The deviations from additive yields were found analogously to Table 4.

For estimation of the synergy characteristics, the function $\ln(\Delta/x_B)$ was plotted versus $\ln(x_A)$ according to Equation (11) in Figure 4. The slopes of the linear trendlines represent directly the values of n, and the reciprocals give logarithms of the synergy factors $\ln(\delta_{n,1})$. Figure 4 demonstrates that the synergy characteristics depend on the blending ratio. An obvious change in the values of the slopes at equivalent shares of components ($\ln x_A = \ln 0.5 = -0.69$) suggests that the process consists of two different synergy reactions described by n > 1 when kerogen prevails (region I), and by n < 1 when wood prevails (region II). The synergy characteristics found are given in Table 7.

The data in Figure 4 and Table 7 show that synergy in the yields of the three products discussed is caused by reaction of 2.6–3.4 moles of kerogen with one mole of wood when kerogen prevails in the blend. When less

Table 7. Polymolar synergy factors and exponents for the yields of co-pyrolysis products

Product	G + w		B + A		B	
	I	II	I	II	I	II
n	2.85(±0.20)	0.49(±0.04)	2.59(±0.18)	0.58(±0.04)	3.44(±0.21)	0.23(±0.06)
$\delta_{n,1}$, %(g/g)$^{-(n+1)}$	−164	−33	200	50	252	28
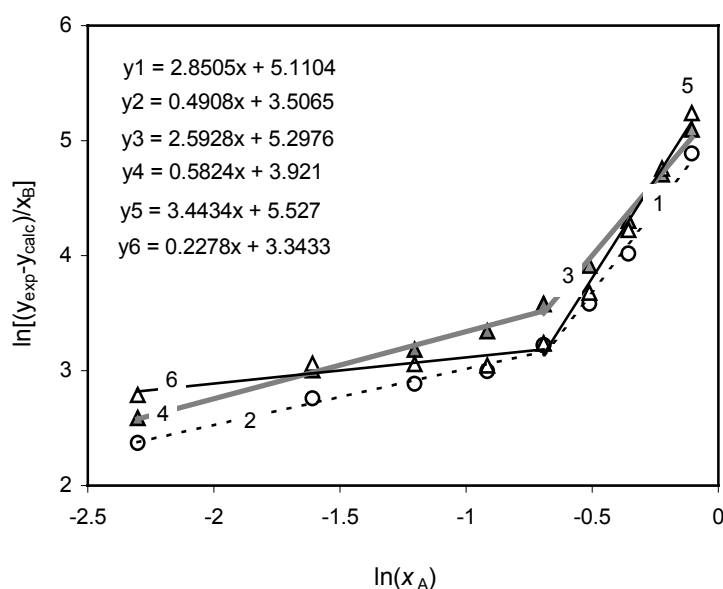
Fig. 4. Trendlines to estimate the polymolar synergy characteristics n and $\delta_{n,1}$ for the yields of co-pyrolysis products: 1 – (G + w)I, 2 – (G + w)II, 3 – (B + A)I, 4 – (B + A)II, 5 – BI, 6 – BII.

kerogen is mixed with prevailing wood, on the contrary, two to four wood moles (1/n) react with one mole of kerogen. It can be supposed that the prevailing component dilutes, separates and protects the formation of associates of the minor component.

4.4. Prediction of the yields of co-pyrolysis products using the polymolar synergy model

Yields of the co-pyrolysis products were predicted introducing the synergy characteristics from Table 7 into the following equation:

$$y_{exp} = \delta_{n,1} (x_A)^n x_B + x_A y_{A1} + x_B y_{B1} \tag{15}$$

The results are depicted in Figure 5. A good accordance is evident between the yields predicted using the polymolar synergy model (15) and experimental yields.
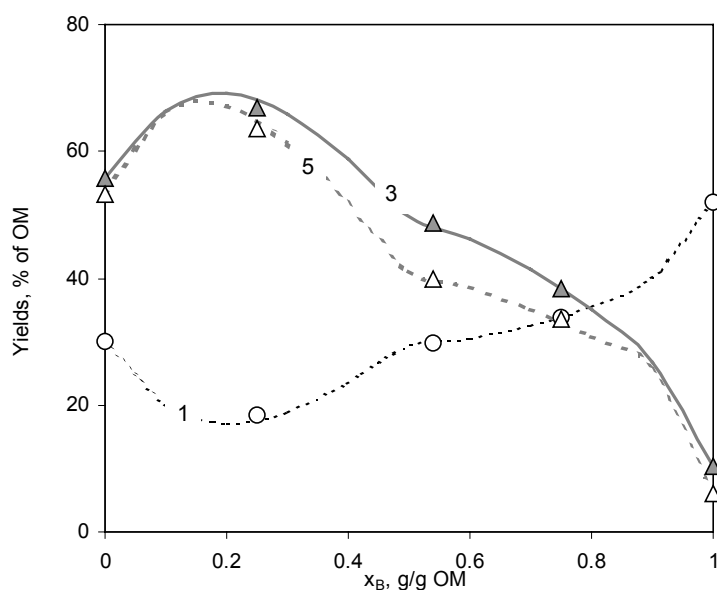
Fig. 5. Effect of blend composition on the yield of co-pyrolysis products assuming polymolar synergy reactions. Points illustrate experimental yields, curves depict the yields predicted according to Equation (15) (symbols see in Fig. 1).

4. 5. Modeling and prediction of the yields of compound groups in benzene extract

According to Table 1, the yield of the benzene solubles from individual oil shale was 53.2% and from individual wood only 6%. So, for discussion of actual contributions of the blend composition to the group composition of the benzene extract, the experimental yields of compounds from Table 2, their interpolated values, the proportional additive yields and synergies were expressed on the basis of total OM in the blends. The coefficients of the second-order polynomial trendlines and the respective yields and synergies are given in Tables 8 and 9.

The trendlines for estimation of synergy factors are presented in Figure 6, and the data obtained in Table 10.

Table 8. Regression coefficients of the second-order polynomial trendlines for the yields of compound groups in benzene extract, % of OM

	Group of compounds	b_2	b_1	b_0
1	High polar heterocompounds	−70	42.9	30.4
2	Neutral heterocompounds	−6.75	−3.83	11.54
3	Polyaromatic hydrocarbons	5.57	−14.5	9.83
4	Monoaromatic hydrocarbons	−1.63	1.09	0.65
5	Nonaromatic hydrocarbons	0.0549	−3.12	3.4

Table 9. Effect of blend composition (g/g) on the yield and synergy of compound groups in benzene extract, % of OM

Blend composition											
x_B, g/g	0.0	0.1	0.2	0.3	0.4	0.5	0.6	0.7	0.8	0.9	1.0
Experimental interpolated yields											
1	28.1	33.99	36.18	36.97	36.36	34.35	30.94	26.13	19.92	12.31	3.8
2	10.9	11.09	10.50	9.78	8.93	7.94	6.81	5.55	4.16	2.63	1.0
3	10.3	8.44	7.15	5.98	4.92	3.97	3.14	2.41	1.79	1.29	0.5
4	0.6	0.74	0.80	0.83	0.83	0.79	0.72	0.61	0.48	0.31	0.2
5	3.2	3.09	2.78	2.47	2.16	1.85	1.55	1.24	0.94	0.64	0.5
Calculated additive yields											
1	28.1	25.71	23.28	20.85	18.42	15.99	13.56	11.13	8.70	6.26	3.8
2	10.9	9.87	8.89	7.90	6.92	5.94	4.96	3.97	2.99	2.01	1.0
3	10.3	9.34	8.36	7.38	6.39	5.41	4.43	3.45	2.47	1.49	0.5
4	0.6	0.59	0.54	0.50	0.45	0.40	0.35	0.30	0.26	0.21	0.2
5	3.2	2.97	2.69	2.42	2.14	1.86	1.59	1.31	1.03	0.76	0.5
Synergies											
1	0.00	8.28	12.90	16.12	17.94	18.36	17.38	15.00	11.22	6.05	0.00
2	0.00	1.22	1.62	1.88	2.01	2.00	1.86	1.58	1.16	0.62	0.00
3	0.00	−0.90	−1.20	−1.39	−1.47	−1.44	−1.30	−1.04	−0.67	−0.19	0.00
4	0.00	0.15	0.26	0.33	0.38	0.39	0.36	0.31	0.22	0.10	0.00
5	0.00	0.12	0.09	0.05	0.02	−0.01	-0.04	−0.07	−0.09	−0.12	0.00
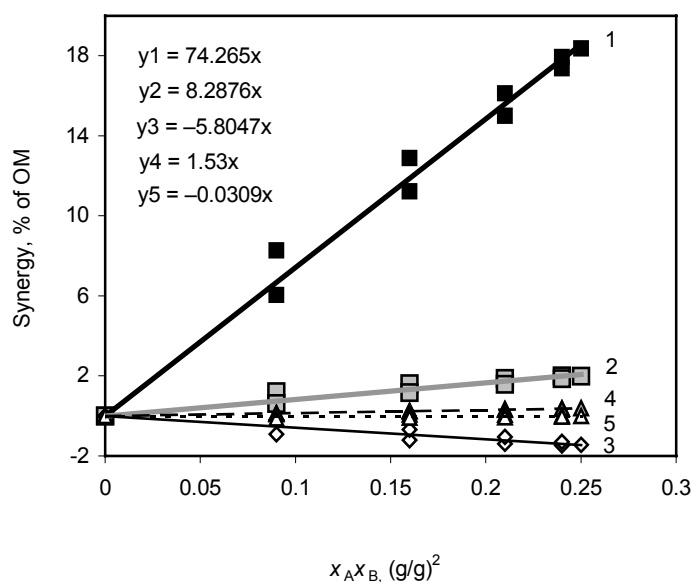
Fig. 6. Trendlines to estimate equimolar synergy factors $\delta_{1,1}$ for the yields of compound groups in the benzene extract: 1 – high polar heterocompounds, 2 – neutral heterocompounds, 3 – polyaromatic hydrocarbons, 4 – monoaromatic hydrocarbons, 5 – nonaromatic hydrocarbons.

Table 10. Equimolar synergy factors for the yields of compound groups in benzene extract

Compound group[1]	1	2	3	4	5
$\delta_{1,1}$, %(g/g)$^{-2}$	74.3	8.29	−5.80	1.53	−0.03
Standard error, ±	1.3	0.36	0.35	0.03	0.13

[1] See in Tables 2 and 8 and Figure 6.

Comparison of the experimental yields of compound groups in the benzene fraction with the values predicted using the model proposed (Equation (14)) is depicted in Figure 7 (curves 1–5).
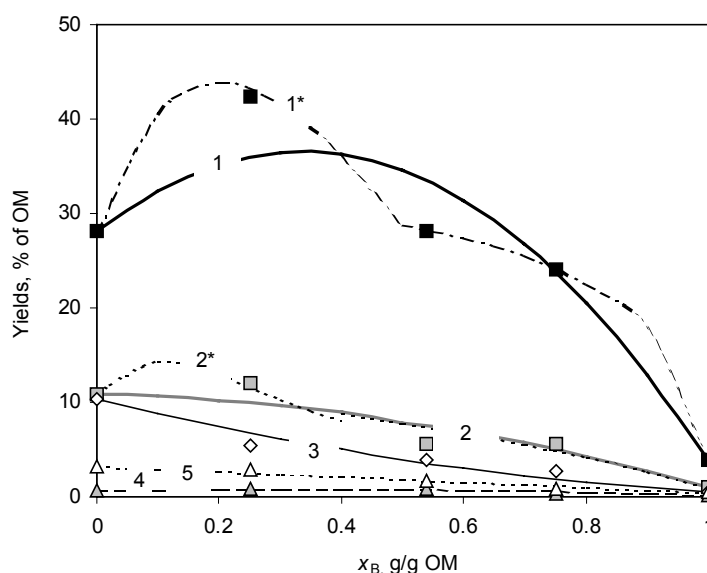
Fig. 7. Effect of blend composition on the yield of compound groups in the benzene extract. Points illustrate experimental yields, curves 1–5 depict the yields predicted for equimolar reactions, and curves 1* and 2* for polymolar reactions (symbols see in Fig. 6).

Assuming that the noticeable deviation of experimental yields of benzene soluble compound groups from the calculated curves 1 and 2 is not caused by experimental errors, an nth-order synergy reaction should take place. So, Equation (11) for polymolar reactions was plotted in Figure 8 to elaborate the synergy characteristics of the groups of heterocompounds 1 and 2.

The synergy characteristics found from the slopes of trendlines in Figure 8 are presented in Table 11.
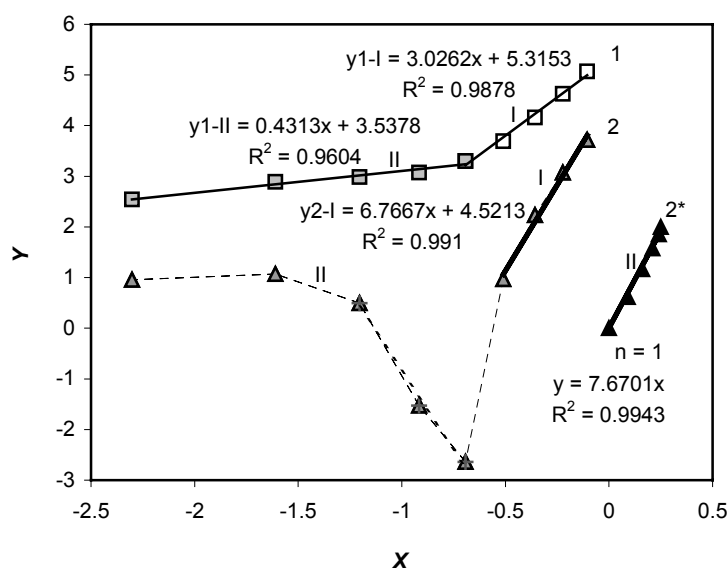
Fig. 8. Trendlines to estimate polymolar synergy characteristics n and $\delta_{n,1}$ ($X = \ln x_A$, $Y = \ln (\Delta/x_B)$) for the yields of high polar (1) and neutral (2) heterocompounds in the blends where kerogen (I) and sawdust (II) prevail, and to estimate $\delta_{1,1}$ ($X = x_1x_2$, $Y = \Delta$) for the yields of neutral heterocompounds when sawdust prevails (2*-II) ($X = x_1x_2$, $Y = \Delta$).

Table 11. Polymolar synergy factors and exponents for the yields of hetero-compounds in benzene extract

Product	High polar heterocompounds		Neutral heterocompounds	
	1-I	1-II	2-I	2*-II
n	3 (±0.2)	0.43(±0.05)	6.8(±0.5)	1
$\delta_{n,1}$, %(g/g)$^{-(n+1)}$	202	34.5	92	7.67(±0.13)

Two different ranges of the blending ratio are obvious for the hetero-compounds. When kerogen prevails (1-I, 2-I), several moles of kerogen are needed for the synergy reaction per mole of wood, like in the synergy characteristics of the total benzene fraction depicted in Figure 4. When wood prevails, only 0.43 mole/mole of kerogen is needed for the high polar compounds (1-II). But a specific curve of neutral heterocompounds (2-II) shows a really trivial polymolar synergy ($8.9*10^{-4}(x_A)^{-6.2}x_B$) between 0.5 and 0.7 g/g of wood. So, it is suggested to apply the equimolar model (2*-II) in the region.

A good accordance is evident from Figure 7 between the yields predicted using the polymolar synergy reaction characteristics from Table 11 and the experimental yields. Besides, the curves in Figure 7 and the synergy factors

in Tables 10 and 11 reveal quantitatively that an essential positive synergy in the yield of benzene soluble oil results predominantly from an additional formation of unwanted high polar heterocompounds (max. by 18%) and neutral heterocompounds (max. by 2%), whereas the synergies are trivial in the yields of welcome hydrocarbons.

5. Conclusions

For the first time, a mathematical model has been proposed to describe the influence of blending ratio on the synergy (Δ) in co-pyrolysis of two components, A and B. The model is based on the stability of a new cross-compound, A_nB, formed between the liquid (solvent soluble) and solid (insoluble) pyrolysis products. A new characteristic, synergy factor ($\delta_{n,1}$), has been introduced to express the synergy formula $\Delta = \delta_{n,1}(x_A)^n x_B$ where x_A and x_B are the shares of components in the blend, and n is the number of A moles reacting with one mole of solid (insoluble) B in the synergy reaction. When A_nB is volatile or soluble in the solvents applied for oil extraction, the synergy is positive, and when insoluble, a negative driftage of the characteristic from the proportionally additive values takes place.

The model deduced has been proved in the mathematical processing of earlier published experimental results [26] on the co-pyrolysis of oil shale and wood blends in supercritical water at 380 °C during 4 hours The values of $\delta_{1,1}$ estimated for the decomposition products decrease in the row, %(g/g)$^{-2}$: sum of benzene and acetone extracts 89.0, water and ether extracts 12.9, solid residue –36.6, and gas and pyrogenetic water –65.4. The values of $\delta_{1,1}$ for the yields of components in the benzene soluble fraction decrease as follows: high polar heterocompounds 74.3, neutral heterocompounds 8.3, monoaromatic hydrocarbons 1.53, aliphatic hydrocarbons –0.03, and polycyclic hydrocarbons –5.8.

Acknowledgements

REFERENCES

1. Di Nola, G., de Jong, W., Spliethoff, H. TG-FTIR characterization of coal and biomass single fuels and blends under slow heating rate conditions: Partitioning of the fuel-bound nitrogen. *Fuel Process. Technol.,* 2010, **91**(1), 103–115.
2. Vuthaluru, H. B. Thermal behaviour of coal/biomass blends during co-pyrolysis. *Fuel Process. Technol.*, 2004, **85**(2–3)**,** 141–155.

3. Ulloa, C. A., Gordon, A. L., García, X. A. Thermogravimetric study of inter-actions in the pyrolysis of blends of coal with radiata pine sawdust. *Fuel Process. Technol.*, 2009, **90**(4)**,** 583–590.

4. Meesri, C., Moghtaderi, B. Lack of synergetic effects in the pyrolytic charac-teristics of woody biomass/coal blends under low and high heating rate regimes. *Biomass Bioenerg.*, 2002, **23**(1), 55–66.

5. Moghtaderi, B., Meesri, C., Wall, T. F. Pyrolytic characteristics of blended coal and woody biomass. *Fuel*, 2004, **83**(6), 745–750.

6. Sonobe, T., Worasuwannarak, N., Pipatmanomai, S. Synergies in co-pyrolysis of Thai lignite and corncob. *Fuel. Process. Technol.*, 2008, **89**(12), 1371–1378.

7. Weiland, N. T., Means, N. C., Morreale, B. D. Product distributions from isothermal co-pyrolysis of coal and biomass. *Fuel,* 2012, **94**, 563–570.

8. Jones, J. M., Kubacki, M., Kubica, K., Ross, A. B., Williams, A. Devolatilisa-tion characteristics of coal and biomass. *J. Anal. Appl. Pyrol.,* 2005, **74**(1–2), 502–511.

9. Haykiri-Acma, H., Yaman, S., Interaction between biomass and different rank coals during co-pyrolysis. *Renew. Energ.,* 2010, **35**(1), 288–292.

10. Zhang, L., Xu, S., Zhao, W., Liu, S. Co-pyrolysis of biomass and coal in a free fall reactor. *Fuel*, 2007, **86**(3), 353–359.

11. Blesa, M. J., Miranda, J. L., Moliner, R., Izquierdo, M. T., Palacios, J. M. Low-temperature co-pyrolysis of a low-rank coal and biomass to prepare smokeless fuel briquettes. *J. Anal. Appl. Pyrol.*, 2003, **70**(2), 665–677.

12. Park, D. K., Kim, S. D., Lee, S. H., Lee, J. G. Co-pyrolysis characteristics of sawdust and coal blend in TGA and a fixed bed reactor. *Bioresource Technol.*, 2010, **101**(15), 6151–6156.

13. Yuan, S., Dai, Z.-H., Zhou, Z.-J., Chen, X.-L., Yu, G.-S., Wang, F.-C. Rapid co-pyrolysis of rice straw and a bituminous coal in a high-frequency furnace and gasification of the residual char. *Bioresource Technol.*, 2012, **109**, 188–197.

14. Cao, Q., Jin, L., Bao, W., Lv, Y. Investigations into the characteristics of oils produced from co-pyrolysis of biomass and tire. *Fuel Process. Technol.* 2009, **90**(3), 337–342.

15. Acar, P., Sinağ, A., Misirlioğlu, Z., Canel, M. The pyrolysis of scrap tire with lignite. *Energ. Source Part A.*, 2011, **34**(3), 287–295.

16. Sharypov, V. I., Beregovtsova, N. G., Kuznetsov, B. N., Cebolla, V. L., Collura, S., Finqueneisel, G., Zimny, T., Weber, J. V. Influence of reaction parameters on brown coal–polyolefinic plastic co-pyrolysis behavior. *J. Anal. Appl. Pyrol.*, 2007, **78**(2), 257–264.

17. Sharypov, V. I., Marin, N., Beregovtsova, N. G., Baryshnikov, S. V., Kuznet-sov, B. N, Cebolla, V. L., Weber, J. V. Co-pyrolysis of wood biomass and synthetic polymer mixtures. Part I: influence of experimental conditions on the evolution of solids, liquids and gases. *J. Anal. Appl. Pyrol.*, 2002, **64**(1), 15–28.

18. Sharypov, V. I., Beregovtsova, N. G., Kuznetsov, B. N., Membrado, L., Cebolla, V. L., Marin, N., Weber, J. V. Co-pyrolysis of wood biomass and synthetic polymers mixtures. Part III: Characterisation of heavy products. *J. Anal. Appl. Pyrol.*, 2003, **67**(2), 325–340.

19. Sharypov, V. I., Beregovtsova, N. G., Kuznetsov, B. N., Baryshnikov, S. V., Cebolla, V. L., Weber, J. V., Collura, S., Finqueneisel, G., Zimny, T. Co-pyrolysis of wood biomass and synthetic polymers mixtures. Part IV: Catalytic pyrolysis of pine wood and polyolefinic polymers mixtures in hydrogen atmosphere. *J. Anal. Appl. Pyrol.*, 2006, **76**(1–2), 265–270.

20. Yang, F.-S., Qu, J.-L., Yang, Z.-Y., Zhou, A.-N. Thermal decomposition behavior and kinetics of composites from coal and polyethylene. *J. China Univ. Mining Technol.,* 2007, **17**(1), 25–29.

21. Suelves, I., Lázaro, M. J., Moliner, R. Synergetic effects in the co-pyrolysis of samca coal and model aliphatic compounds studied by analytical pyrolysis. *J. Anal. Appl. Pyrol.*, 2002, **65**(2), 197–206.

22. Tiikma, L. *Utilization of Plastic Wastes with Oil Shale.* ISBN 978-3-8433-5019-8. LAP Lambert Academic Publishing AG, Saarbrücken, Germany, 2010. http://www.superbookshop.net/covers/198/9783843350198.jpg

23. Tiikma, L., Luik, H., Pryadka, N. Co-pyrolysis of Estonian shales with low-density polyethylene. *Oil Shale*, 2004, **21**(1), 75–85.

24. Aboulkas, A., El Harfi, K., Nadifiyine, M., El Bouadili, A. Investigation on pyrolysis of Moroccan oil shale/plastic mixtures by thermogravimetric analysis. *Fuel Process. Technol.*, 2008, **89**(11), 1000–1006.

25. Aboulkas, A., Makayssi, T., Bilali, L., El Harfi, K., Nadifiyine, M., Benchanaa, M. Co-pyrolysis of oil shale and plastics: Influence of pyrolysis parameters on the product yields. *Fuel Process. Technol.*, 2012, **96**, 209–213.

26. Veski, R., Palu, V., Kruusement K. Co-liquefaction of kukersite oil shale and pine wood in supercritical water. *Oil Shale,* 2006, **23**(3), 236–248.

27. Zhang, Qi, Chang, Jie, Wang, Tiejun, Xu, Ying. Review of biomass pyrolysis oil properties and upgrading research. *Energ. Convers. Manage.*, 2007, **48**(1), 87–92.